

Prolonged QT intervals in mice with cardiomyocyte-specific deficiency of the molecular clock

Lisa A. Gottlieb^{1,2} | Karin Larsen¹ | Ganesh V. Halade³ | Martin E. Young⁴ | Morten B. Thomsen¹ 

¹Department of Biomedical Sciences, University of Copenhagen, Denmark

²Department of Experimental Cardiology, Amsterdam University Medical Center, locatie AMC, Amsterdam, the Netherlands

³Division of Cardiovascular Sciences, Department of Medicine, University of South Florida, Tampa, FL, USA

⁴Department of Medicine, University of Alabama at Birmingham, AL, USA

Correspondence

Morten B. Thomsen, Cardiac Electrophysiology Group, Department of Biomedical Sciences, University of Copenhagen, Blegdamsvej 3B, Panum 12-5-36, DK-2200 Copenhagen N, Denmark. Email: mbthom@sund.ku.dk

Funding information

Novo Nordisk Fonden, Grant/Award Number: NNF18OC0032728; Carlsbergfondet, Grant/Award Number: CF15-0109; Michaelsen Fonden

Abstract

Aim: Cardiac arrhythmias and sudden deaths have diurnal rhythms in humans. The underlying mechanisms are unknown. Mice with cardiomyocyte-specific disruption of the molecular clock genes have lower heart rate than control. Because changes in the QT interval on the electrocardiogram is a clinically used marker of risk of arrhythmias, we sought to test if the biological rhythms of QT intervals are dependent on heart rate and if this dependency is changed when the molecular clock is disrupted.

Methods: We implanted radio transmitters in male mice with cardiomyocyte-specific Bmal1 knockout (CBK) and in control mice and recorded 24-h ECGs under diurnal and circadian conditions. We obtained left ventricular monophasic action potentials during pacing in hearts ex vivo.

Results: Both RR and QT intervals were longer in conscious CBK than control mice (RR: 117 ± 7 vs 110 ± 9 ms, $P < .05$; and QT: 53 ± 4 vs 48 ± 2 ms, $P < .05$). The prolonged QT interval was independent of the slow heart rate in CBK mice. The QT interval exhibited diurnal and circadian rhythms in both CBK and control mice. The action potential duration was longer in CBK than in control mice, indicating slower repolarization. Action potential alternans occurred at lower pacing rate in hearts from CBK than control mice (12 ± 3 vs 16 ± 2 Hz, respectively, $P < .05$).

Conclusion: The bradycardic CBK mice have prolonged ventricular repolarization independent of the heart rate. Diurnal and circadian rhythms in repolarization are preserved in CBK mice and are not a consequence of the 24-h rhythm in heart rate. Arrhythmia vulnerability appears to be increased when the cardiac clock is disrupted.

KEYWORDS

chronobiology, circadian rhythm, heart rate, mouse model, QT interval, telemetry

1 | INTRODUCTION

There is a morning surge in sudden cardiac death,^{1,2} and several clinical studies have identified a time-of-day dependency in cardiac arrhythmia.³⁻⁶ The underlying mechanisms linking chronobiology to cardiac arrhythmogenesis

are poorly described. Biological rhythms with a wavelength of approximately 24 hours allow the organism to adapt behaviour and physiology in anticipation of an active phase or a sleep phase. Biological clocks maintaining such rhythms have been identified in all investigated mammalian species and in all cell types of the human body, including

cardiomyocytes.⁷ The rhythm is *circadian* in the absence of temporal cues from the environment, whereas *diurnal* rhythms are present when the biological 24-h clocks are entrained by external Zeitgebers, eg, light/dark or food availability.⁷ The suprachiasmatic nucleus in the hypothalamus governs the synchronization of the peripheral clocks to the environmental time via endogenous cues,⁸ eg, body temperature,⁹ glucocorticoid release¹⁰ or neuronal signalling to the target organ.¹¹

The molecular clock is an autonomous cellular mechanism that maintains a circadian rhythm in gene expression, even in the absence of synchronization cues from the suprachiasmatic nucleus. In the heart, 6–13% of all expressed genes are regulated by the molecular clock and have a circadian pattern of expression.^{12–14} One key element of the molecular clock is the transcription factor brain-muscle arnt-like 1 (BMAL1; also known as aryl hydrocarbon receptor nuclear translocator-like 1 protein [ARNTL]). Its function has important implications for cardiac metabolism and contractility: Cardiomyocyte-specific *Bmal1* knockout (CBK) in mice causes impaired ketone body metabolism, depressed glucose utilization, dilated cardiomyopathy, increased fibrosis and reduced cardiac pump function after 28 weeks of life.^{13,15,16}

The cardiac molecular clock can be rendered non-functional in mice by various means, and to our knowledge, they all produce bradycardia relative to wild-type controls.^{17–20} Moreover, changing the 24-h period of the ambient light to 22.5 or 27 hours also slows heart rate significantly in mice but does not change the amplitude of the 24-h rhythm.²¹

The QT interval is dependent on heart rate in most species, and in the mouse, it prolongs about 2 ms for every 10 ms prolongation of the RR interval.²² We have previously described both diurnal and circadian rhythms in QT intervals in wild-type control mice,²² but it is not known if the 24-h rhythm in QT interval is dependent on the 24-h rhythm in heart rate. Because QT interval is an important clinical marker of ventricular repolarization and risk of arrhythmias, we wanted to test if the QT interval is changed in mice with disrupted cardiac molecular clock and to determine if this change is because of the relative bradycardia in these mice. We hypothesized that cardiac repolarization in CBK mice was prolonged independently of a slower heart rate. The perspective of such a finding is a contribution to the mechanistic understanding of the time-of-day dependent risk of fatal ventricular arrhythmias.

2 | RESULTS

Six-lead electrocardiograms (ECG) from 10-wk-old anaesthetized CBK and control mice were compared (Figure 1A). The morphology of the T wave is different in CBK mice:

They have a more pronounced negative part after the QRS complex in lead I, II and aVL (Figure 1B). We found a trend towards slower heart rate in CBK mice, but QT intervals and QT intervals mathematically “corrected” to a heart rate of 600 beats/min (QTc) were comparable (Figure 1C). The mean cardiac axis was similar in CBK and control mice (54 ± 14 vs $59 \pm 26^\circ$; $P = .6$). The ECG of the control mice is comparable to that of age-matched control C57BL6 wild-type mice (data not shown).

2.1 | Diurnal rhythms in RR and QT interval

We evaluated diurnal and circadian rhythms in cardiac repolarization using telemetric devices in CBK and control mice and recorded ECG and activity for five consecutive days. Both CBK and control mice show a peak in physical activity immediately after the onset of the dark phase (Figure 2A), and this peak is also observed during the circadian dark:dark (D:D) cycle (Figure 2B). Exemplary one-lead telemetric ECGs from conscious CBK and control mice are shown in Figure 3A. Figure 3B shows preserved diurnal (left) and circadian (right) rhythms in the RR and QT intervals in CBK mice. RR intervals are shortest, and thus heart rate is faster, during the active phase of the animals. The sinusoidal fits to these data sets show that conscious CBK mice have an overall slower heart rate and a small, but significant, prolongation of the QT interval relative to conscious control (Figure 3B and Table 1). The 24-hours averages of QT intervals are longer in conscious mice (Table 1) compared to the QT interval of the anesthetized animals (Figure 1), despite comparable RR intervals. Notwithstanding, it is clear that diurnal and circadian rhythms in RR and QT intervals are present in control mice and that they are preserved in mice with a non-functional myocardial molecular clock (Figure 3B).

TABLE 1 Analysis of ECG from conscious mice during 24 h

	CBK	Control	P value
n, mice	11	8	—
RR interval, ms	117 ± 7	110 ± 9	.041
PR interval, ms	38 ± 2	38 ± 1	.8
QRS interval, ms	10 ± 1	11 ± 1	.1
QT interval, ms	53 ± 4	48 ± 2	.003
QTc, ms	49 ± 4	46 ± 1	.017

Note: Mean \pm standard deviation. P values from a Student's *t* test after test for normal distribution using Shapiro-Wilk's test. Heart-rate correction of the QT interval (QTc) according to Mitchell.⁴⁴ Recordings made in the light:dark cycle is presented here.

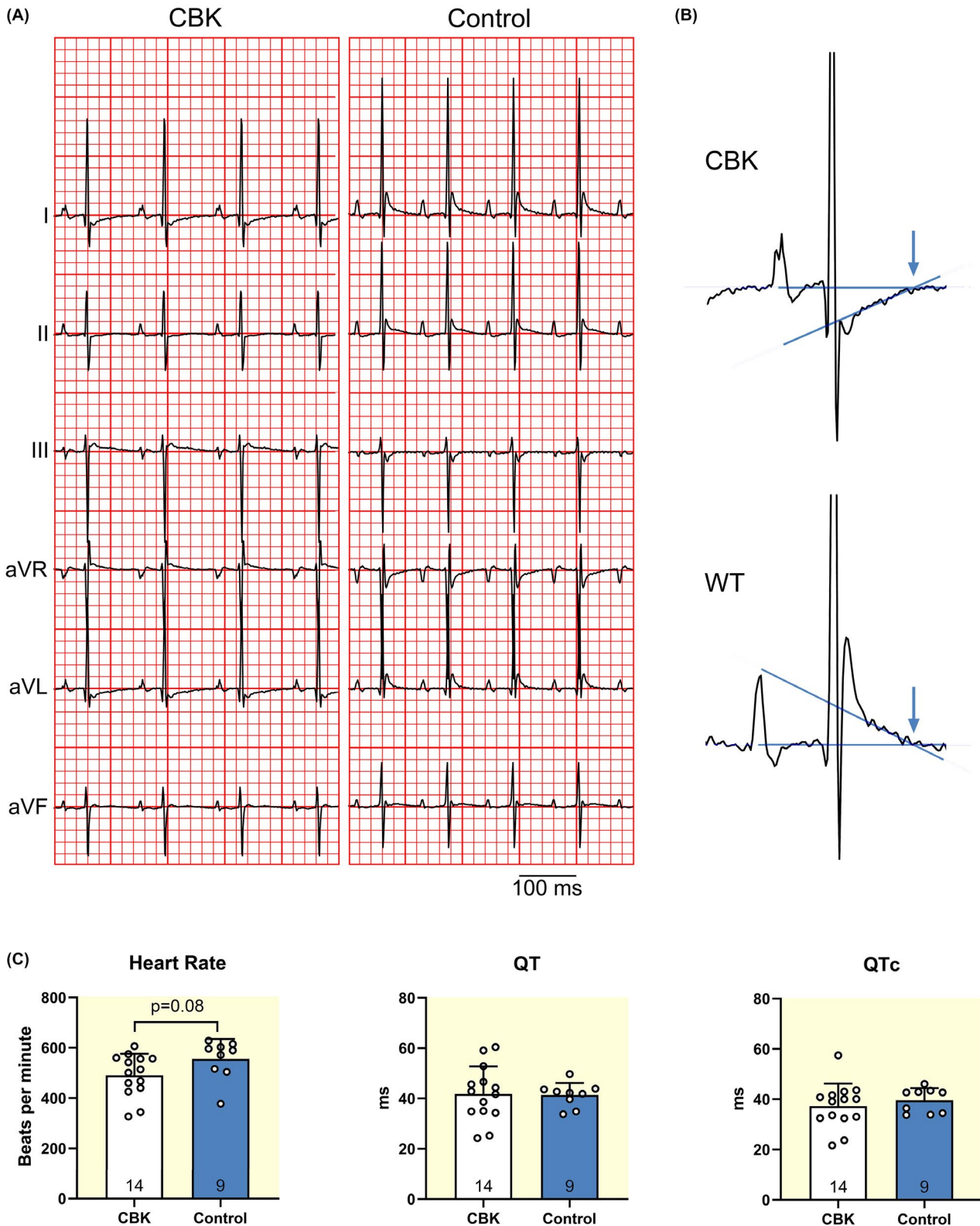


FIGURE 1 A, Exemplary 6-lead ECG traces from a CBK and a control mouse measured under anaesthesia during their inactive phase (ZT = 3–5 h). Note the difference in T-wave morphology. B, ECG complexes on enlarged time and amplitude axes to illustrate how the end of the T wave was determined at the intercept between the isoelectric line and the tangent to the last part of the T wave. Downward arrows indicate the end of the T wave used for the measurement of QT interval. C, Heart rate, QT interval and heart-rate corrected QT intervals (QTc) in anesthetized CBK and control mice. The number of animals is noted and the error bars represents the mean \pm standard deviation. *P* value based on a Student's *t* test

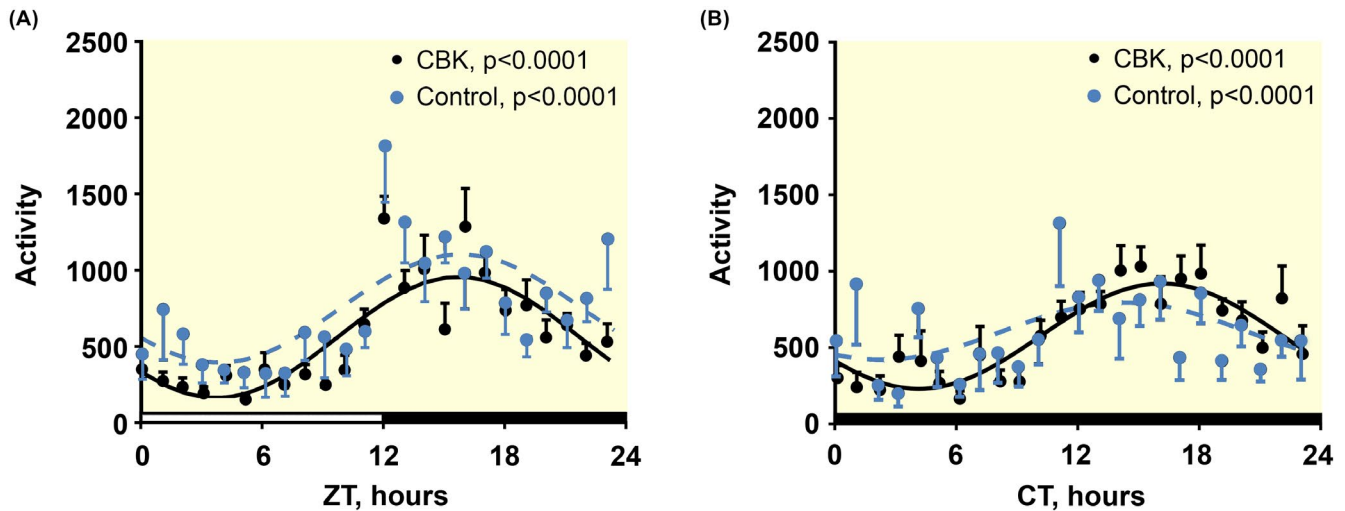


FIGURE 2 A, Diurnal rhythms in physical activity in CBK and control mice. Activity in the horizontal plane was measured in arbitrary units. ZT is Zeitgeber time, where ZT = 0 is the time cue, ie, lights on at 6 AM. B, Circadian rhythms in physical activity in CBK and control mice. CT is circadian time, where CT = 0 indicates the extrapolated subjective onset of the day (ie, at 6 AM, but the light remains off). *P* values <.05 indicate a statistical acknowledgement of a 24-h rhythm (*n* = 8 control mice and 11 CBK mice). Parameters from the cosinor fits are reported in Table S1

2.2 | Heart-rate variability

We determined time-domain parameters of heart rate variability (HRV) over the 24-hours period in light:dark (L:D; Table 2). This analysis confirmed the relative bradycardia in CBK mice and showed comparable indices of HRV. Moreover, the size of the Poincaré plot of all beats was comparable in CBK and control mice (short- and long-axis SD; Table 2). The relative power was smaller in the low-frequency band and larger in

TABLE 2 Heart-rate variability analysis of ECG from conscious mice during 24 h

	CBK	Control	<i>P</i> value
n, mice	11	8	—
RR interval, ms	120 ± 8	108 ± 6	.003
SDRR, ms	22.4 ± 4.4	20.0 ± 2.6	.2
pRR6, %	22 ± 12	18 ± 7	.7
Short-axis SD, ms	8.0 ± 4.7	5.9 ± 2.2	.3
Long-axis SD, ms	30.4 ± 5.7	27.6 ± 3.7	.2
Low frequency, %	18.8 ± 6.6	27.1 ± 8.4	.028
High frequency, %	38.7 ± 18.7	19.2 ± 8.6	.014

Note: Mean ± standard deviation. All RR intervals of the 24-h period were used (range: 553,182–792,129 beats) for the time-series analysis. *P* values from an unpaired Student's *t* test. SDRR, standard deviation of the RR intervals. pRR6, percentage of successive RR interval differences longer than 6 ms. Short- and long-axis SD, standard deviation of all RR intervals projected on the short and long axes of the Poincaré plot, respectively. The Poincaré plot displays all RR intervals vs the next RR interval. The long axis is the line of identity ($x = y$) of the Poincaré plot, and the short axis is perpendicular to this line. Frequency analyses were made based on the recommendations from Thireau et al.⁴⁵ Analysis of recordings made in the light:dark cycle is presented here.

the high-frequency band in CBK mice than in control mice, suggesting a higher parasympathetic tone in CBK mice, which also may explain the relative bradycardia in these mice.

2.3 | Heart-rate correction of QT

The diurnal and circadian rhythms in QT intervals may simply be a function of the 24-h cycle in heart rate. Given the many shortcomings of QT_c,²² we took an alternate approach to determine if the 24-h QT-RR relationship is causal. Given our continuous 24-h recordings, we had >500,000 ECG complexes on file per mouse. We found the mean RR interval in each mouse and averaged all ECG complexes within a 1 ms range of this RR interval in the mouse each hour and measured the QT intervals (Figure 4A). There was a clear 24-hours rhythm of the QT interval in control mice, which was independent of the 24-hours RR rhythm and preserved in CBK mice. A similar analysis was performed in D:D, and comparable results were obtained (Table S1).

The longer QT intervals in CBK mice may be because of the relative bradycardia. The average RR interval in all the mice was 115±8ms (*n* = 19), so we selected all ECG complexes with an RR interval between 114 and 116 ms (Figure 4B). The corresponding QT intervals showed statistically significant 24-hours rhythm (Figure 4B), and the average QT interval was longer in CBK mice (56.9 ± 0.2 ms in CBK vs 50.8 ± 0.2 ms in control mice, *P* < .001). Thus, there are diurnal and circadian rhythms in the QT interval independent of the 24-hours cycle in heart rate in CBK and control mice, and the bradycardia is not the underlying reason for QT prolongation in CBK mice.

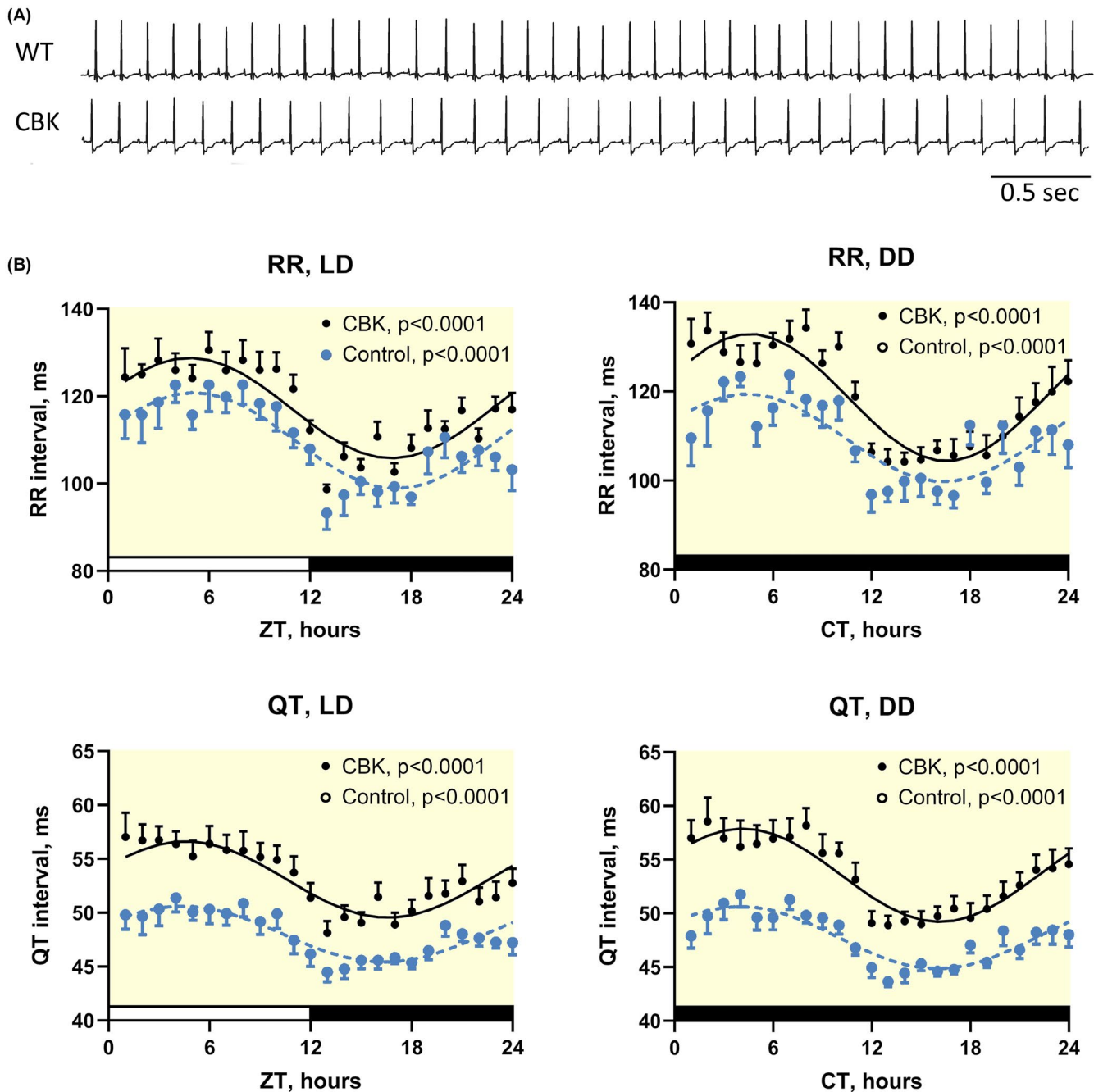


FIGURE 3 A, Five-second exemplary traces from telemetry recordings during the light phase from a control and a CBK mouse. B, Diurnal and circadian rhythms in RR and QT intervals in control and CBK mice. Diurnal rhythms were recorded in light:dark phase (L:D), whereas circadian rhythms were recorded in dark:dark phase (D:D). Data presented as mean \pm standard deviation. P values $< .05$ indicate a statistical acknowledgement of a 24-h rhythm ($n = 8$ control mice and 11 CBK mice). The 24-h means of these parameters are given in Table 1. Parameters from the cosinor fits are reported in Table S1

2.4 | Action-potential duration and alternans

Next, we evaluated intrinsic heart rate and repolarization duration in isolated, spontaneously beating hearts. In this preparation, the parasympathetic system nor other neurohumoral factors influence the heart. Coronary flow was comparable in CBK and control hearts (not shown), and all hearts were

in sinus rhythm. The intrinsic heart rate was comparable in hearts from CBK and control hearts (Figure 5A). Action potential duration (APD), here quantified to 50 and 90% repolarization (APD₅₀ and APD₉₀, respectively) were also similar in CBK and control hearts (Figure 5B). The hearts were paced at the right ventricle from 7 Hz (420 beats/min, 143 ms interpulse interval) to the fastest possible frequency with 1:1 capture. APD₉₀ shortened when pacing frequency

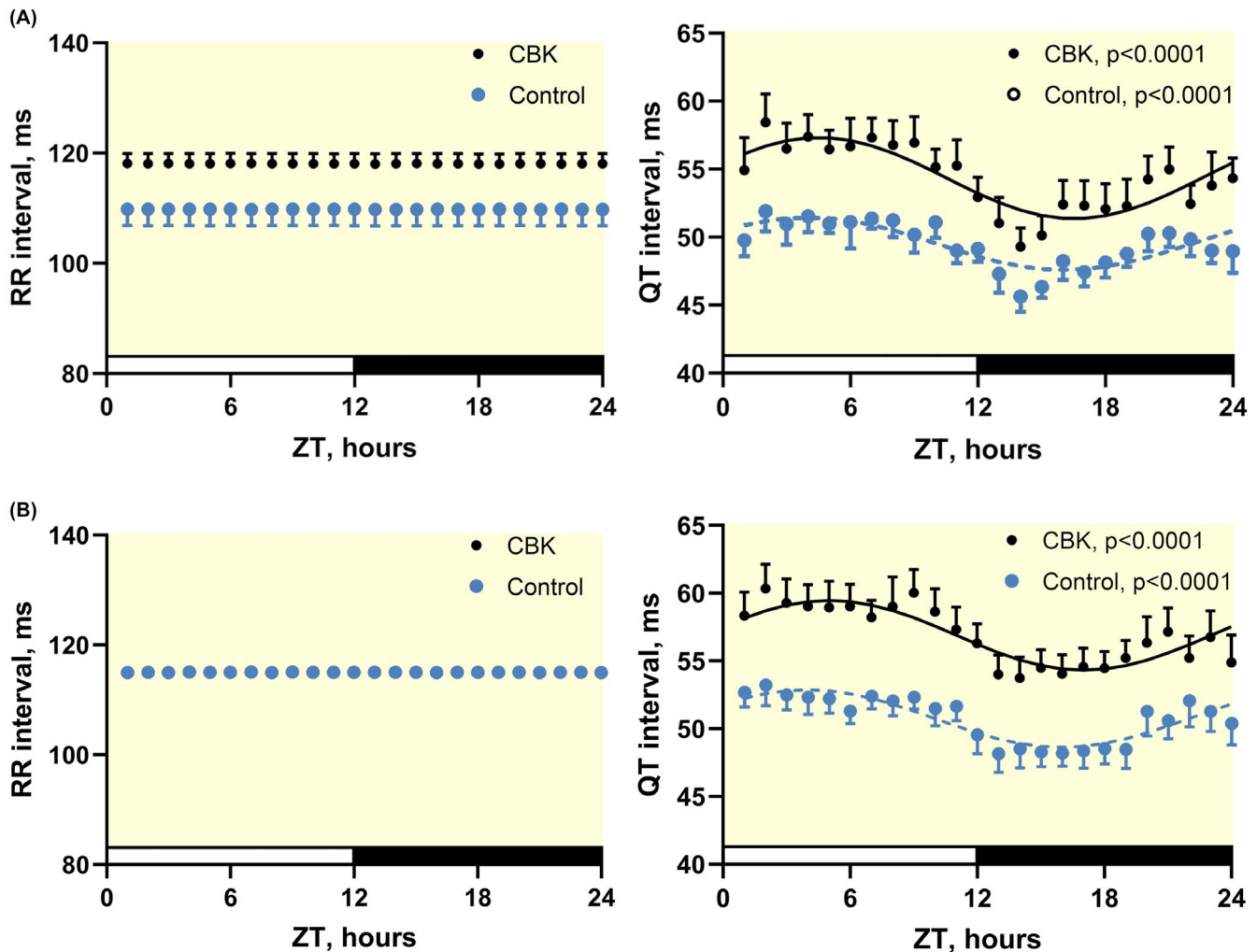


FIGURE 4 A, ECG complexes were selected with an RR interval within 1 ms of the 24-h mean RR of the individual mouse (left panel). QT intervals were then determined each hour from these selected complexes only (right panel). The resulting 24-h rhythms in QT intervals are statistically significant ($P < .05$) in the absence of any 24-h rhythm in RR interval. B, ECG complexes were selected with an RR interval between 114 and 116 ms, the overall mean RR interval of all mice (left panel). The QT intervals displayed 24-h rhythms in both CBK and control animals. Group sizes: 8 control mice and 11 CBK mice. Parameters from the cosinor fits are reported in Table S1

was increased in all hearts (Figure 5C). Moreover, APD was longer in hearts from CBK mice compared to hearts from control mice ($P = .0029$; Figure 5C). Linear regression to the restitution curves revealed comparable slopes but a higher intercept in CBK (data not shown). The action potential repolarization slope between 10 and 40 ms after the action potential peak was significantly more flat in paced CBK hearts (Figure 5D). When progressively increasing pacing rates from 7 Hz, 5/10 control hearts and 4/9 CBK hearts developed action potential alternans ($P = 1.0$); however, alternans developed earlier, at a slower pacing frequency in CBK mice (11.5 ± 3 vs 16.0 ± 2 Hz, $P = .04$ [Mann-Whitney test]; Figure 5E). Figure 5F shows an exemplary trace of 32 action potentials with overt alternans. Thus, CBK hearts have

slower repolarization during pacing, and they are more vulnerable to alternans.

3 | DISCUSSION

In the present study, we observed a prolongation in QT interval independent of RR interval in conscious mice with cardiomyocyte-specific deficiency in the molecular clock that was associated with a longer action potential duration and increased vulnerability to ventricular alternans. Moreover, these mice had a slower heart rate that may be explained by increased activity of the parasympathetic system, as suggested by HRV analysis.

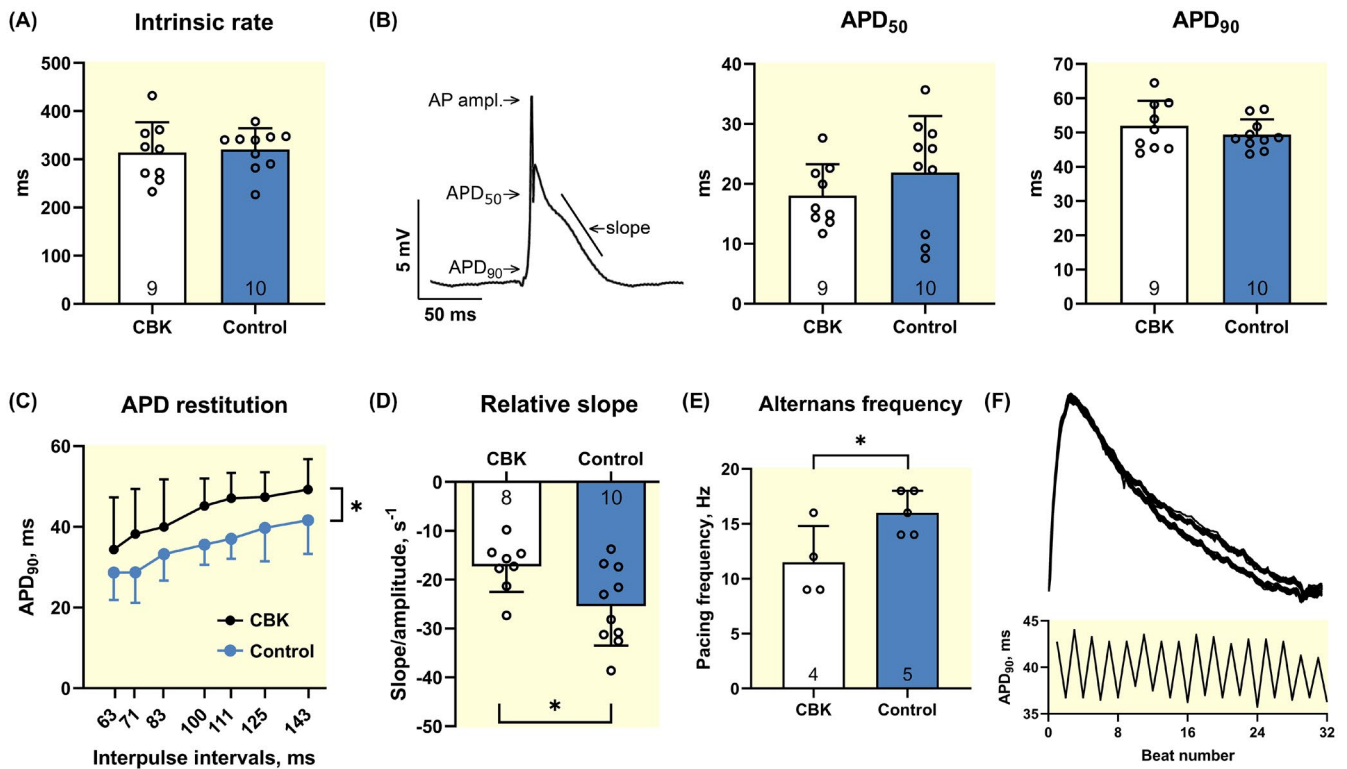


FIGURE 5 A, Intrinsic sinus rate is comparable in isolated, perfused hearts from CBK and control mice. B, Exemplary monophasic action potential showing measurements of action potential (AP) amplitude (AP ampl.); AP duration to 50% (APD₅₀) and to 90% (APD₉₀) repolarization; and the fitted slope to the linear phase of the repolarization between 10 and 40 ms after the AP upstroke. The bar graphs show APD₅₀ and APD₉₀ during sinus rhythm. C, APD₉₀ during ventricular pacing from 7 Hz (143 ms interpulse interval) to 16 Hz (63 ms interpulse interval). A mixed-effect, repeated measures statistical model indicated an effect of pacing frequency ($P < .0001$) and genotype ($*P = .029$). D, Repolarizing slope relative to AP amplitude during 7 Hz pacing. E, Pacing frequency at which AP alternans develops, which occurred in only 5 control and 4 CBK hearts. Number of hearts noted in the bars, which represent the mean \pm standard deviation. Asterisks (*) in panels D and E indicate a P value $< .05$ based on a Student's t test. F, A representative example of pacing-induced alternans: 32 consecutive APs superimposed to show alternans on the latter half of the AP. Lower panel shows APD₉₀ of the 32 APs, showing an alternans amplitude of 6-7 ms

3.1 | Slow heart rate in CBK mice

Heart rate is determined by the cardiac sinus node and is orchestrated by the combined action of i) proteins involved in calcium cycling across sarcoplasmic reticulum and sarcolemma membranes, ii) ion channels and iii) the autonomic nervous system. There is a day-night difference in the expression of *Hcn4* encoding the primary ion channel for pacemaking and a larger HCN4-governed depolarizing current in sinus-node cells acutely isolated from control mice at the beginning of the dark phase compared to the beginning of the light phase.²³ This is very likely a key underlying mechanism of the 24-h variation in heart rate; however, the preservation of this 24-h cycle in CBK mice in the present study suggests that other mechanisms compensate for HCN4 when the cardiac molecular clock is eliminated. Only when *Bmal1* is eliminated in the entire mouse, the diurnal variation in heart rate is lost.¹⁹

A slower heart rate may also be secondary to an increased sensitivity of the sinus node towards the tone of

the parasympathetic nervous system. In the present study, we find increased power in the high-frequency band and reduced power in the low-frequency band in conscious CBK mice, suggesting that the CBK heart is indeed more sensitive to parasympathetic stimulation. Notwithstanding, significant doubt has been raised regarding the reliability of HRV analysis when making conclusions about the vagal tone, especially when rate changes.^{24,25} Swoap et al have shown an unchanged diurnal heart rate profile in muscarinic type 2 receptor knockout mice²⁶; however, at heart rates in control and knockout animals significantly faster than in the present study. During isoflurane anaesthesia, heart rate was numerically slower in CBK mice (Figure 1B), but this did not reach statistical significance. The difference in heart rate completely disappears ex vivo when the heart is denervated (Figure 5A) lending support to the hypothesis of increased parasympathetic sensitivity in the CBK heart. Irrespective of the underlying mechanism(s), it is now well established by the present and other studies^{17,18,20,27} that conscious mice with disrupted cardiac molecular clocks

have slower heart rates *in vivo*, but the 24-hours rhythmicity is preserved.

3.2 | Longer repolarization in CBK mice

We report that QT intervals have a 24-h cycle in conscious control mice and that this is preserved when controlling for the 24-h cycle in heart rate. Moreover, we show QT *in vivo* and APD *ex vivo* are prolonged in CBK mice compared to control mice, and that this is not secondary to the relative bradycardia in CBK mice.

QT interval duration exhibit diurnal rhythms and heart-rate ‘correction’ of QT intervals (QTc) imperfectly flattens the 24-h cycle.²⁸ Similarly, mice have diurnal and circadian rhythms in QT intervals (Figure 3 and reference²⁹) and by selecting ECG complexes in a very limited range of RR intervals, we show a preserved 24-h QT cycle without the use of mathematical correction formulas (Figure 4). Moreover, there is a general prolongation of cardiac repolarization *in vivo* and *ex vivo* that is independent of heart rate. Cardiac repolarization quantified by the QT interval is an intricate balance between depolarizing (Na⁺ and Ca²⁺) and repolarizing (K⁺) ionic currents. Any change in a current density will change repolarization and QT-interval duration. Ion channels governing depolarization are comparable for humans and mice; however, because of the faster heart rate of the mouse, faster repolarization and shorter QT intervals are necessary. Kv11.1 and Kv7.1 are the ion channels active in human repolarization, whereas Kv1.4, Kv1.5, Kv2.1 and Kv4.2 are among the ion channels involved in the murine repolarization.^{30–32} Tong *et al* found 24-h rhythms in the expression of genes encoding Kv1.5, Kv2.1 and Kv4.2 in mice, which were lost upon the autonomic blockade.³³ Schroder and colleagues confirmed the circadian expression of the gene coding for Kv4.2 and also found a 24-h cycle in mRNA for Kir2.1 and Nav1.5 in mice.¹⁸ The latter is an ion channel producing a depolarizing sodium current and could underlie a circadian variation in QRS duration, which we showed previously.²² Circadian variation in a Kv4.2 accessory subunit, KCHIP2, was suggested to underlie the 24-h cycle in QT intervals³⁴; however, we were not able to reproduce this finding in KCHIP2-deficient mice.²² Hearts from control mice have a circadian expression of KCNH2 encoding Kv11.1, an ion channel that opens late in the (human) action potential and contributes significantly to repolarization. Also, inducible CBK mice lose the circadian expression of KCNH2,²⁹ raising the possibility that Kv11.1 may be physiologically relevant in mice.

A diurnal rhythm in QT intervals is present in patients with a cardiac pacemaker, even when the pacemaker is programmed to a constant heart rate of 70 beats/min for

24 hours.³⁵ Contrary, when patients with a completely denervated heart after cardiac transplant are studied, the 24-h cycle in QT intervals is absent.³⁵ This corroborates our findings in mice that the 24-hours QT cycle is independent of heart rate and supports the hypothesis that the autonomic nervous system is important for maintaining the 24-hours QT cycle.

Ex vivo, we find a prolonged action potential duration in CBK hearts when they are paced electrically to maintain constant heart rate (Figure 5C) and an increased vulnerability to AP alternans when pacing frequency is increased (Figure 5E,F). This appears to be in conflict with a recent publication where isolated CBK hearts are reported to be protected against pacing-induced arrhythmias.²⁰ There is a day-night difference in AP alternans susceptibility which is lost at ageing³⁶ and sinus node arrhythmias and conduction block in inducible CBK mice¹⁸; however, this is unlikely a result of compromised repolarization, yet underscores the increased arrhythmia susceptibility when disrupting the cardiac clock.

3.3 | Perspectives and limitations

These findings add to the large collection of chronobiological literature strongly suggesting that time of day is taken into account when designing and interpreting experimental and clinical studies, including electrophysiological testing and pharmacological interventions. The morning surge in sudden cardiac death¹ and in ventricular extra beats⁶ may be related to the independent 24-h cycle in QT intervals, rather than a change in heart rate.

The present study only investigated male mice at a narrow age range of 9–11 weeks. QT intervals are longer in humans, in females and vary with the estrus cycle.³⁷ It will be interesting to describe the superimposed effects of the 24-h circadian rhythm and murine 4-day estrus cycle on cardiac electrophysiology. Moreover, our method did not consider the presence of QT–RR hysteresis, in which acceleration and deceleration of the heart rate generate either longer or shorter QT intervals, respectively.³⁸ We made the assumption that the mice had similar periods of increased activity (heart rate acceleration) and subsequent recovery (heart rate deceleration) within each analyzed hour, thus generating a mean QT interval.

In conclusion, heart rate and QT intervals follow a 24-h cycle in control mice, and the diurnal variation in QT is independent of the 24-h rhythm in heart rate. The diurnal variation in QT interval is preserved in CBK mice. Repolarization duration is prolonged in the bradycardic CBK mice *in vivo* and *ex vivo*, and this QT prolongation is not a consequence of the relative bradycardia. Arrhythmia vulnerability appears to be increased when the cardiac clock is disrupted.

4 | MATERIALS AND METHODS

4.1 | Animals and ethical approvals

All experiments were carried out in accordance with the European Union legislation for the protection of animals used for scientific purposes (Directive 2010/63/EU). Experiments in Copenhagen were performed under license from The Ministry of Food, Agriculture and Fisheries, Denmark. The local Institutional Animal Care and Use Committees approved all experiments. The mice were based on crossing *Bmal1*^{fl_{ox}/fl_{ox}} mice (B6.129S4(Cg)-*Arntl*^{tm1^{Wei}/J}, Jackson Laboratory, ME, USA) with heterozygote cardiac-specific alpha myosin-heavy chain-driven *Cre* recombinase transgenic mice, *Cre*^{+/-} (B6N.FVB(B6)-Tg(Myh6-*Cre*)2182Mds/J, Jackson Laboratory, ME, USA). CBK mice were *Cre*^{+/-}, whereas littermate control mice were *Bmal1*^{fl_{ox}/fl_{ox}} and *Cre*^{-/-}. Genotyping was performed in-house or commercially (GeneTyper, NY, USA). Only male mice at 9-11 weeks of age were used for these experiments. Mice were housed at constant 22°C in a 12-hours light/dark schedule (lights on at 6 AM; zeitgeber time (ZT) 0) and provided with food and tap water ad libitum.

4.2 | Surface electrocardiograms

Six-lead surface ECG was measured for 10 minutes during full anaesthesia (2% isoflurane in O₂) in 23 mice in the diurnal time-of-day interval ZT3-5h (inactive phase). Electrodes were placed subcutaneously in antibrachial and femoral regions, and signals were recorded at 4 kHz. QT interval was measured in lead I (Figure 1). Body temperature was monitored and kept at 36-37°C during all recordings. All mice received a telemetry implant after the ECG recording.

4.3 | Telemetry

Under complete anaesthesia (2% isoflurane in O₂), telemetric devices (ETA-F10, DataSciences International, MN, USA) were implanted subcutaneously on the back region between the scapulas as described previously.^{22,39} Body temperature was monitored and kept at 36-37°C during the entire procedure. Subcutaneous carprofen (10 mg/kg) and a lidocaine-bupivacaine mix (0.4 mg/kg and 1.0 mg/kg, respectively) were administered to all mice in the subcutaneous device pocket for post-operative analgesia.

Mice were left >1 week to fully recover from the surgery. We excluded 4 mice because of lead dislodgement and poor ECG quality. Hereafter, we recorded ECG (at 1 kHz) and movements of the mouse in the cage in the horizontal plane continuously for 5 days where the mice were conscious and

freely roaming in their home cage. During the first 24 hours, mice were exposed to 12 hours light (6 AM-6 PM) and 12 hours complete darkness (6 PM-6 AM) in alignment with their previous exposure in the animal facilities. Next, the light was turned off for a total of 96 hours. The ambient light was recorded at 1 Hz simultaneously with the ECG recordings. The mice are considered to be in diurnal (L:D) rhythm for the first 24 hours and in circadian (D:D) rhythm for the last 24 hours of the 96-hours dark period. Drifting of the circadian phase is observed after several weeks of constant darkness and is therefore not considered being present in the relatively short time interval of our studies.⁴⁰ The implanted telemetric devices sent the ECG signal to a receiver (RPC-1) placed underneath the animal cage. The signals were converted by an analogue output adaptor and a data acquisition device (Option R08 and PowerLab 8/30, respectively; ADInstruments, Dunedin, New Zealand) and recorded on a standard computer using LabChart (ADInstruments, Dunedin, New Zealand).

4.4 | Isolated heart studies

Twenty-three male mice were killed at ZT 4-7, the hearts were quickly excised and the aorta retrogradely perfused with a modified Krebs-Henseleit solution (in mmol/L: 118 NaCl, 4.7 KCl, 1.75 CaCl₂, 1.2 KH₂PO₄, 1.2 Mg₂SO₄, 24.9 NaHCO₃, 11.0 glucose; 37°C; pH = 7.4). The solution was continuously equilibrated with a mixture of 5% CO₂ and 95% O₂. Perfusion pressure was set to 70-75 mmHg, and hearts with a resulting coronary flow of 0.7-4.0 mL/min and an intrinsic heart rate in sinus rhythm between 200 and 500 beats/min were included in the study. Moreover, we analysed coronary autoregulation by changing the perfusion pressure by 20 mmHg.⁴¹ Only hearts that responded with a change in flow <0.75 mL/min were included in the study. Based on these criteria, four hearts were excluded from the study.

A single, monophasic action potential catheter was placed on the left mid-ventricular epicardium and adjusted so the recorded action potential amplitude was >8 mV at the beginning of the study. A pacing catheter was placed on the epicardium of the right ventricle and current impulses (1 ms duration) were provided by an external, isolated stimulator (DS3, Digitimer, Welwyn Garden City, UK) controlled by the LabChart software. The excitation threshold was determined by gradually increasing current amplitude until cardiac capture. The pacing was delivered at twice the threshold for >1 minute at each frequency from lowest possible to 20 Hz.

4.5 | Analysis

Activity and ECG were analysed using LabChart as previously described.^{22,42,43} Activity was measured in the two

mice groups to evaluate the timing of the active phase. QT intervals were mathematically corrected to a heart rate of 600 beats/min ($QT_c = QT/(RR/100)^{1/2}$; all variables in milliseconds) as proposed by Mitchell et al.⁴⁴

Heart-rate variability (HRV) was analysed in the time domain from all RR intervals for 24 hours in L:D as suggested by Thireau et al.⁴⁵ We calculated the mean RR interval, the standard deviation of the RR intervals (SDRR) and the percentage of successive RR interval differences longer than 6 ms (pRR6). Poincaré plots were made displaying all RR intervals vs the next RR interval,⁴⁶ and the standard deviation of all RR intervals projected on the short and long axes of the Poincaré plot were determined. The long axis is the line of identity ($x = y$) in the Poincaré plot, and the short axis is perpendicular to this line. The frequency-domain parameters of HRV were analyzed using 3×3 -minutes epochs, as suggested by Thireau et al.⁴⁵ at ZT = 3, 4 and 5 h which correspond to the inactive phase (cf. Figure 2). Frequency bands were 0.15-1.5 Hz for low frequency (LF) and 1.5-5.0 Hz for high frequency (HF).

Duration of the monophasic action potentials from upstroke to 50 and 90% repolarization (APD_{50} and APD_{90} , respectively) was determined in LabChart during sinus rhythm and ventricular pacing. In addition, we determined the slope of the repolarization between 10 and 40 ms after the upstroke and report this relative to the action potential amplitude. The presence of action potential alternans was determined from visual inspection of APD_{90} plotted as a function of beat number. The slowest pacing frequency which produced action potential alternans was noted for each heart.

4.6 | Statistical analysis

Data for all tables, Figures 1 and 5, were tested for normal distribution using Shapiro-Wilk's test and presented as mean \pm standard deviation. When relevant, we display the individual data points of all biological replicates superimposed on bar graphs. In figures with 24 hours on the x-axis (Figures 2-4), we depict the mean value and standard deviation of the parameter for each hour. The regression fits in the figures are obtained from applying a cosine model⁴⁷ to all 24-h data in the given group, obtaining the chronobiological rhythm parameters amplitude, mesor and acrophase. The period was set to 24 hours. The parameters obtained from the fit are reported in Table S1. We applied an F test to the fitted chronobiological parameters to test the presence of an overall diurnal or circadian rhythm in the electrophysiological parameters. We rejected the null hypothesis (amplitude is zero) when $P < .05$ and thereby accepting the presence of a rhythm. This P value is given in the figure panels. Statistical comparison of electrophysiological parameters from CBK and control mice were done using Student's t tests or mixed-effect, repeated measures statistical model, as indicated in figure legends. Alternans inducibility

was compared using a Mann-Whitney test. P values less than .05 are considered to be statistically significant.

ACKNOWLEDGEMENTS

LAG was supported by the Michaelsen Foundation. This work was supported by the Carlsberg Foundation (CF15-0109) and the Novo Nordisk Foundation (NNF18OC0032728). The data that support the findings of this study are available from the corresponding author upon reasonable request.

CONFLICT OF INTEREST

The authors have no conflict of interest.

ORCID

Morten B. Thomsen  <https://orcid.org/0000-0002-2469-6458>

REFERENCES

- Muller JE, Ludmer PL, Willich SN, et al. Circadian variation in the frequency of sudden cardiac death. *Circulation*. 1987;75(1):131-138.
- Willich SN, Levy D, Rocco MB, Tofler GH, Stone PH, Muller JE. Circadian variation in the incidence of sudden cardiac death in the Framingham Heart Study population. *Am J Cardiol*. 1987;60(10):801-806.
- Yamashita T, Murakawa Y, Sezaki K, et al. Circadian variation of paroxysmal atrial fibrillation. *Circulation*. 1997;96(5):1537-1541.
- O'Mahony C, Lambiase PD, Rahman SM, et al. The relation of ventricular arrhythmia electrophysiological characteristics to cardiac phenotype and circadian patterns in hypertrophic cardiomyopathy. *Europace*. 2012;14(5):724-733.
- Aizawa Y, Sato M, Ohno S, et al. Circadian pattern of fibrillatory events in non-Brugada-type idiopathic ventricular fibrillation with a focus on J waves. *Heart Rhythm*. 2014;11(12):2261-2266.
- Ruwald MH, Moss AJ, Zareba W, et al. Circadian distribution of ventricular tachyarrhythmias and association with mortality in the MADIT-CRT trial. *J Cardiovasc Electrophysiol*. 2015;26(3):291-299.
- Golombek DA, Rosenstein RE. Physiology of circadian entrainment. *Physiol Rev*. 2010;90(3):1063-1102.
- Ralph MR, Mrosovsky N. Behavioral inhibition of circadian responses to light. *J Biol Rhythms*. 1992;7(4):353-359.
- Buhr ED, Yoo S-H, Takahashi JS. Temperature as a universal resetting cue for mammalian circadian oscillators. *Science (New York, NY)*. 2010;330(6002):379-385.
- Balsalobre A, Brown SA, Marcacci L, et al. Resetting of circadian time in peripheral tissues by glucocorticoid signaling. *Science (New York, NY)*. 2000;289(5488):2344-2347.
- Dibner C, Schibler U, Albrecht U. The mammalian circadian timing system: organization and coordination of central and peripheral clocks. *Annu Rev Physiol*. 2010;72:517-549.
- Storch K-F, Lipan O, Leykin I, et al. Extensive and divergent circadian gene expression in liver and heart. *Nature*. 2002;417(6884):78-83.
- Martino T, Arab S, Straume M, et al. Day/night rhythms in gene expression of the normal murine heart. *J Mol Med*. 2004;82(4):256-264.

14. Zhang R, Lahens NF, Ballance HI, Hughes ME, Hogenesch JB. A circadian gene expression atlas in mammals: implications for biology and medicine. *Proc Natl Acad Sci USA*. 2014;111(45):16219-16224.
15. Young ME, Brewer RA, Pelicciari-Garcia RA, et al. Cardiomyocyte-specific BMAL1 plays critical roles in metabolism, signaling, and maintenance of contractile function of the heart. *J Biol Rhythms*. 2014;29(4):257-276.
16. Ingle KA, Kain V, Goel M, Prabhu SD, Young ME, Halade GV. Cardiomyocyte-specific Bmal1 deletion in mice triggers diastolic dysfunction, extracellular matrix response, and impaired resolution of inflammation. *Am J Physiol Heart Circ Physiol*. 2015;309(11):H1827-1836.
17. Bray MS, Shaw CA, Moore MWS, et al. Disruption of the circadian clock within the cardiomyocyte influences myocardial contractile function, metabolism, and gene expression. *Am J Physiol-Heart Circ Physiol*. 2008;294(2):H1036-H1047.
18. Schroder EA, Lefta M, Zhang X, et al. The cardiomyocyte molecular clock, regulation of Scn5a, and arrhythmia susceptibility. *Am J Physiol Cell Physiol*. 2013;304(10):C954-965.
19. Curtis AM, Cheng Y, Kapoor S, Reilly D, Price TS, FitzGerald GA. Circadian variation of blood pressure and the vascular response to asynchronous stress. *PNAS*. 2007;104(9):3450-3455.
20. Hayter EA, Wehrens SMT, Van Dongen HPA, et al. Distinct circadian mechanisms govern cardiac rhythms and susceptibility to arrhythmia. *Nat Commun*. 2021;12(1):2472.
21. West AC, Smith L, Ray DW, Loudon ASI, Brown TM, Bechtold DA. Misalignment with the external light environment drives metabolic and cardiac dysfunction. *Nat Commun*. 2017;8(1):417.
22. Gottlieb LA, Lubberding A, Larsen AP, Thomsen MB. Circadian rhythm in QT interval is preserved in mice deficient of potassium channel interacting protein 2. *Chronobiol Int*. 2017;34(1):45-56.
23. D'Souza A, Wang Y, Anderson C, et al. A circadian clock in the sinus node mediates day-night rhythms in Hcn4 and heart rate. *Heart Rhythm*. 2021;18(5):801-810.
24. Marmarstein JT, McCallum GA, Durand DM. Direct measurement of vagal tone in rats does not show correlation to HRV. *Sci Rep*. 2021;11(1):1210.
25. Monfredi O, Lyashkov AE, Johnsen A-B, et al. Biophysical characterization of the underappreciated and important relationship between heart rate variability and heart rate. *Hypertension*. 2014;64(6):1334-1343.
26. Swoap SJ, Li C, Wess J, Parsons AD, Williams TD, Overton JM. Vagal tone dominates autonomic control of mouse heart rate at thermoneutrality. *Am J Physiol Heart Circ Physiol*. 2008;294(4):H1581-1588.
27. Lefta M, Campbell KS, Feng H-Z, Jin J-P, Esser KA. Development of dilated cardiomyopathy in Bmal1-deficient mice. *Am J Physiol-Heart Circ Physiol*. 2012;303(4):H475-H485.
28. Singh I, Rabkin SW. Circadian variation of the QT interval and heart rate variability and their interrelationship. *J Electrocardiol*. 2021;65:18-27.
29. Schroder EA, Burgess DE, Zhang X, et al. The cardiomyocyte molecular clock regulates the circadian expression of Kcnh2 and contributes to ventricular repolarization. *Heart Rhythm*. 2015;12(6):1306-1314.
30. Grubb S, Speerschneider T, Occhipinti D, et al. Loss of K⁺ currents in heart failure is accentuated in KCHIP2 deficient mice. *J Cardiovasc Electrophysiol*. 2014;25(8):896-904.
31. Marionneau C, Brunet S, Flagg TP, Pilgram TK, Demolombe S, Nerbonne JM. Distinct cellular and molecular mechanisms underlie functional remodeling of repolarizing K⁺ currents with left ventricular hypertrophy. *Circ Res*. 2008;102(11):1406-1415.
32. Nerbonne JM, Kass RS. Molecular physiology of cardiac repolarization. *Physiol Rev*. 2005;85(4):1205-1253.
33. Tong M, Watanabe E, Yamamoto N, et al. Circadian expressions of cardiac ion channel genes in mouse might be associated with the central clock in the SCN but not the peripheral clock in the heart. *Biol Rhythm Res*. 2013;44(4):519-530.
34. Jeyaraj D, Haldar SM, Wan X, et al. Circadian rhythms govern cardiac repolarization and arrhythmogenesis. *Nature*. 2012;483(7387):96-99.
35. Bexton RS, Vallin HO, Camm AJ. Diurnal variation of the QT interval—influence of the autonomic nervous system. *Br Heart J*. 1986;55(3):253-258.
36. Wang Z, Tapa S, Francis Stuart SD, et al. Aging disrupts normal time-of-day variation in cardiac electrophysiology. *Circul Arrhythmia Electrophysiol*. 2020;13(9):e008093.
37. Saito T, Ciobotaru A, Bopassa JC, Toro L, Stefani E, Eghbali M. Estrogen contributes to gender differences in mouse ventricular repolarization. *Circ Res*. 2009;105(4):343-352.
38. Pelchovitz DJ, Ng J, Chicos AB, Bergner DW, Goldberger JJ. QT-RR hysteresis is caused by differential autonomic states during exercise and recovery. *Am J Physiol Heart Circ Physiol*. 2012;302(12):H2567-2573.
39. Thomsen MB, Nielsen MS, Aarup A, Bisgaard LS, Pedersen TX. Uremia increases QRS duration after β -adrenergic stimulation in mice. *Physiol Rep*. 2018;6(13):e13720.
40. Eckel-Mahan K, Sassone-Corsi P. Phenotyping circadian rhythms in mice. *Curr Protoc Mouse Biol*. 2015;5(3):271-281.
41. Bayliss WM. On the local reactions of the arterial wall to changes of internal pressure. *J Physiol (Lond)*. 1902;28(3):220-231.
42. Speerschneider T, Thomsen MB. Physiology and Analysis of the Electrocardiographic T Wave in Mice. *Acta Physiol (Oxf)*. 2013;209(4):262-271.
43. Speerschneider T, Grubb S, Metoska A, Olesen S-P, Calloe K, Thomsen MB. Development of heart failure is independent of KCHIP2 expression. *J Physiol (Lond)*. 2013;591(23):5923-5937.
44. Mitchell GF, Jeron A, Koren G. Measurement of heart rate and Q-T interval in the conscious mouse. *Am J Physiol*. 1998;274(3):H747-751.
45. Thireau J, Zhang BL, Poisson D, Babuty D. Heart rate variability in mice: a theoretical and practical guide. *Exp Physiol*. 2008;93(1):83-94.
46. Thomsen MB, Verduyn SC, Stengl M, et al. Increased short-term variability of repolarization predicts d-sotalol-induced torsades de pointes in dogs. *Circulation*. 2004;110(16):2453-2459.
47. Nelson W, Tong YL, Lee JK, Halberg F. Methods for cosinorhythmometry. *Chronobiologia*. 1979;6(4):305-323.

SUPPORTING INFORMATION

Additional Supporting Information may be found online in the Supporting Information section.

How to cite this article: Gottlieb LA, Larsen K, Halade GV, Young ME, Thomsen MB. Prolonged QT intervals in mice with cardiomyocyte-specific deficiency of the molecular clock. *Acta Physiol*. 2021;233:e13707. <https://doi.org/10.1111/apha.13707>